Organic "Paleothermometers": Long-chain ketones (alkenones) and glycerol dialkyl glycerol tetraethers (GDGTs) as SST indicators

General Reading:

- Eglinton T.I. and Eglinton G. (2008) Molecular proxies for paleoclimatology. *Earth Planet. Sci. Lett.* **275**, 1-16.

Targeted Reading:

Alkenones:

- Brassell S.C., Eglinton G., Marlowe I.T., Pflaumann U. and Sarnthein M. (1986) Molecular Stratigraphy: A new tool for climatic assessment. *Nature*, **320**, 129-133.
- F.G. Prahl and Wakeham S.G. (1987) Calibration of unsaturation patterns in long-chain ketone compositions for paleotemperature assessment. *Nature*, **330**, 367-369.
- Muller P.J., Kirst G., Ruhland G., von Storch I. And Rosell-Mele (1998) Calibration of the alkenone paleotemperature index UK37' based on core-tops from the eastern southern South Atlantic and the global ocean (60°N-60°S). Geochmi. Cosmochim. Acta 62, 1757-1772.
- Proceedings of a workshop on alkenone-based paleoceanographic indicators (www.g-cubed.org, 2000).

GDGTs

- Schouten S., Hopmans E.C., Schefuss E. and Sinninghe Damste J.S. (2002) Distributional variations in marine crenarchaeotal membrane lipids: a new tool for reconstructing ancient sea water temperatures? EPSL 204 265-274.
- Weijers W.H., Schouten S., van den Donker J.C., Hopmans E.C. and Sinninghe Damste J.S. (2007) Environmental controls on bacterial tetraether membrane lipid distribution in soils. GCA 71 703-713.

The alkenone story - birth of a novel paleoceanographic tool

1978

Boon et al., 1978

- First identification in sediments
- DSDP core from Walvis Ridge, SW Africa
- Technique: field desorption-MS of total lipid extract and TLC fractions
- Identified as ketones with elemental compostion of $C_{37}H_{70}O$ (m/z 530) and $C_{38}H_{72}O$ (m/z 544)

1980

de Leeuw et al. 1980

- Confirmation of structure as C_{37}-C_{39} methyl and ethyl ketones in sediments.

Volkman et al. 1980

- Identification of same compounds in *Emiliania huxleyi*
- Feeding experiments reveal conservative behavior on passage through gut of zooplankton and excretion as fecal pellets
- Identification of associated compounds (C_{31}-C_{38} odd-chain alkenes) in *E. huxleyi*
- Formed throughout growth cycle of *E. huxleyi*
- Proposed as markers for *E. hux.*

Walvis Ridge sediments,
SE Atlantic
Boon et al., 1978

Thin-layer chromatography

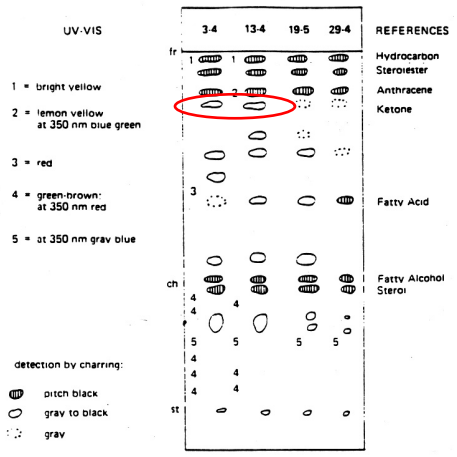

Field desorption-MS of Total Lipid Extract
("soft" ionization method)

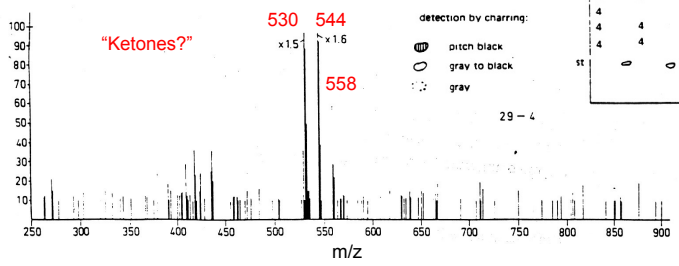

Alkenones – Magical Molecules!

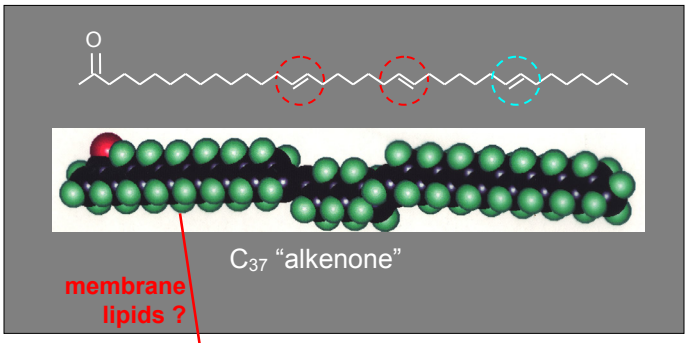

C_{37} "alkenone"

membrane lipids ?

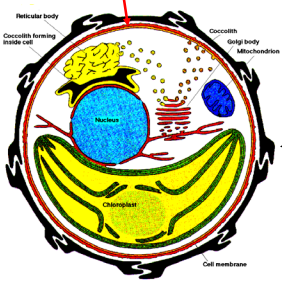

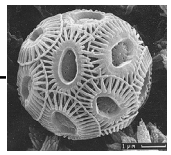

Photomicrograph of E. Huxleyi

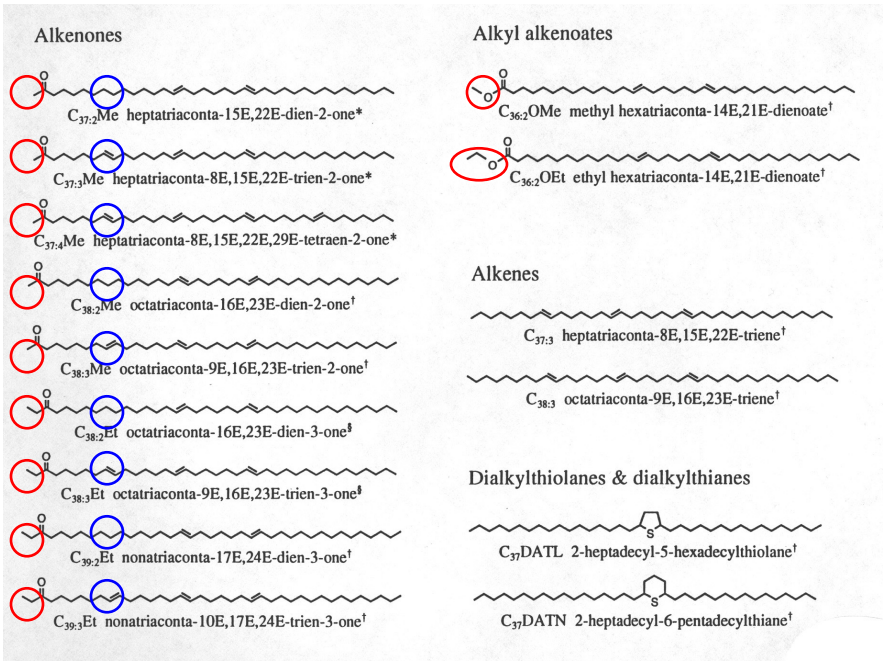

Emiliania huxleyi

Affiliation and Evolution

- Class: Haptophyta (Prymnesiophyta)
- Order: Isochrysidales
- Family: Gephyrocapsaceae
- *E. huxleyi* first appeared during late Pleistocene (ca. 250ka)

Distribution and Abundance

- Cosmopolitan eurythermal species (sub-polar to equatorial regions).
- Often found in high concentrations (up to $5x10^3$ l^{-1}).
- Occasional development of dense blooms.
- Most widespread extant coccolithophoric species.
- Dominant in transitional and subarctic floral zones.
- Isochrysis/Chrysotila limited to coastal environments.
- *E. huxleyi* considered to be the dominant source of alkenones in the open ocean.
- Constitutes between 40-87% and 40-67% of coccoliths in surface sediments in the North Atlantic and Pacific oceans respectively.

Some Definitions:

Class:
- A taxonomic group containing one or more orders.

Order:
- A taxonomic group containing one or more families.

Family:
- A taxonomic group containing one or more genera.

Genus (pl. Genera):
- The second most specific taxonomic level, includes closely related species. Interbreeding between organisms within the same genus can occur.

Species:
- A taxonomic category subordinate to a genus (or subgenus) composed of individuals possessing common characters distinguishing them from other categories of individuals of the same taxonomic level. In taxonomic nomenclature, species are designated by the genus name followed by a Latin or Latinised adjective or noun.
- A taxonomic group whose members can interbreed.

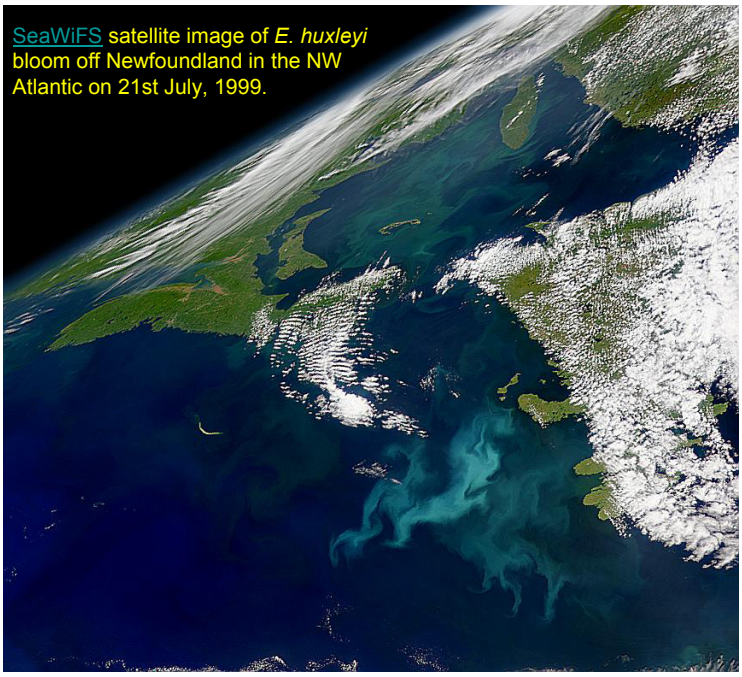

Emiliania huxleyi

Morphology and Composition
- 2 distinct morphotypes
- warm water form and cold water form

Alkenone characteristics
- long chain-length (C_{37}-C_{39})
- spacing of positions of unsaturation (C-7 not C-2 and C-3)
- double-bond configuration (i.e. *E* not *Z; trans* not *cis*)
- major components of living cell carbon (5-11%)

Other features
- Co-occurring methyl and ethyl alkenoates
- C_{31}-C_{37} odd carbon number alkenes
- Carotenoid: 19'-hexanoyloxyfucoxanthin
- Unusual water-soluble acidic polysaccharide

Long-chain ketones

- Recognized in three genera of prymnesiophycean algae
- Emiliania
- Chrysotila
- Isochrysis

Biosynthesis and biological role
- Algae biosynthesize alkenones from CO_2 via a C_{36} alkenoic acid precursor (Volkman et al., 1980)
- Precise biological role not known
- May play serve as membrane fluidity regulators (lipid bilayer)
- "margarine vs butter" analogy

Occurrence
- Identified in sediments from a wide variety of depositional environments (see table)
- Also identified in freshwater (lacustrine) sediments
- Occur in POM in Atlantic and Pacific oceans
- Found in remote marine aerosols collected on New Zealand (introduced into the atmosphere by bubble bursting - Sicre et al., 1990)

The alkenone story - birth of a novel paleoceanographic tool

1984
Marlowe et al 1984
- Alkenones found to be common to Prymnesiophyceae
- Alkyl alkenoates found as associated compounds
- Chemotaxonomic value confirmed
- Degree of unsaturation related to growth temperature

1985
Cranwell et al. 1985
- Alkenones identified in freshwater lake sediments

1986
Farrimond et al. 1986
- Alkenones reported in Cretaceous black shales
- Demonstrates additional biological precursor for alkenones since this pre-dates appearance of *E. huxleyi*.

Brassell et al., 1986
- Relationship in degree of unsaturation and $\delta^{18}O$ observed
- Proposal as a molecular marker for sea-surface temperature
- Introduction of parameter, U^{K}_{37}
- Correlation between latitude, SST and U^{K}_{37} in Quaternary sediments
- Introduction to the concept of ***molecular stratigraphy***

Farrimond et al. 1986

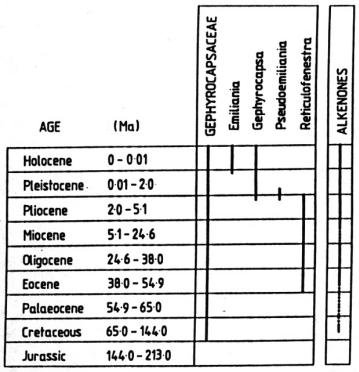

AGE	(Ma)
Holocene	0 - 0·01
Pleistocene	0·01 - 2·0
Pliocene	2·0 - 5·1
Miocene	5·1 - 24·6
Oligocene	24·6 - 38·0
Eocene	38·0 - 54·9
Palaeocene	54·9 - 65·0
Cretaceous	65·0 - 144·0
Jurassic	144·0 - 213·0

GEPHYROCAPSACEAE: Emiliania; Gephyrocapsa; Pseudoemiliania; Reticulofenestra

ALKENONES

Fig. 5. Geological age ranges of genera belonging to the family Gephyrocapsaceae, and the reported sedimentary occurrence of long-chain alkenones. (Modified from Marlowe *et al.*, 1985). The dotted lines reflect age ranges where alkenones have not been reported from sediments.

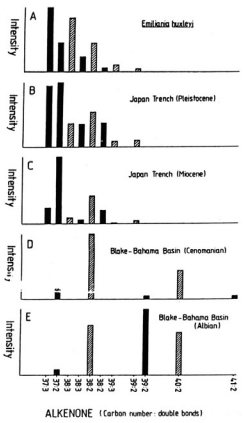

Gas chromatograph of TLE of Kane Gap sediments

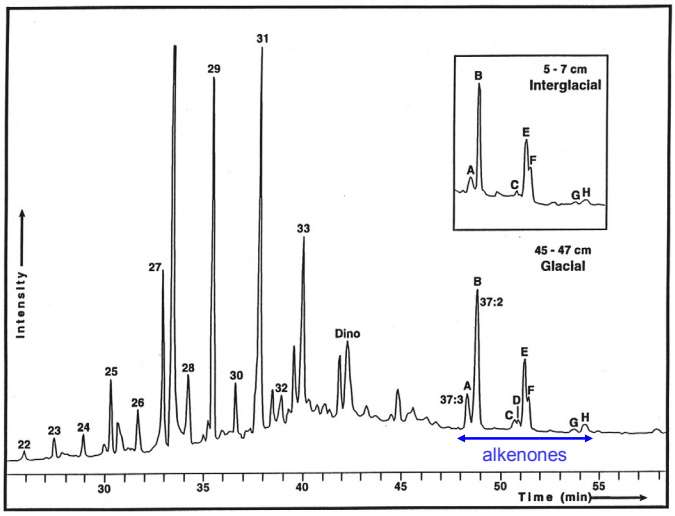

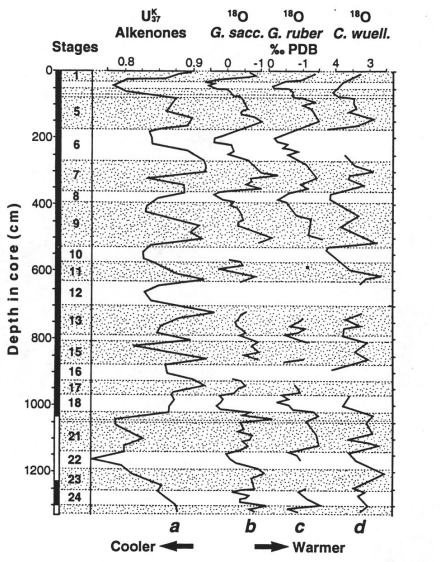

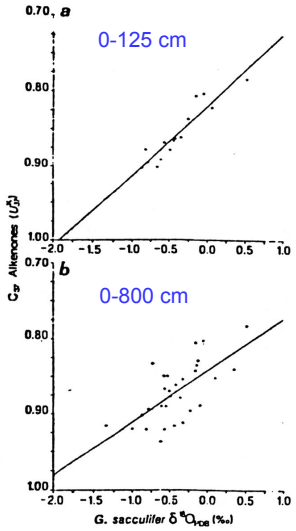

Brassell et al., 1986

Latitudinal variations in U^K_{37} values of sediments and particulate samples

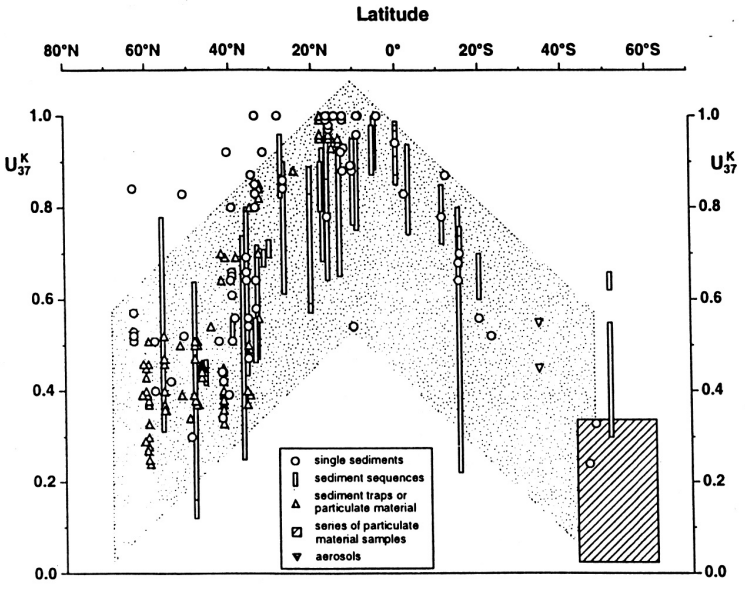

Brassell et al., 1986

The alkenone story - birth of a novel paleoceanographic tool

1987

Prahl and Wakeham, 1987

- Calibration of Uk37' w.r.t. SST for natural POM populations (sinking and suspended) in Atlantic and Pacific oceans

1988

Prahl et al, 1988

- Calibration of Uk37 vs laboratory cultures of E. huxleyi (commonly accepted calibration)
- Confirm systematic changes in
- degree of unsaturation
- overall chain length distribution
- proportion in alkyl alkenoates/alkenones

Rechka and Maxwell, 1988

- Complete structural assignment of alkenones
- Found to be unusual all *E* (trans-) configuration
- Refractory nature postulated to be related to unusual double-bond configuration

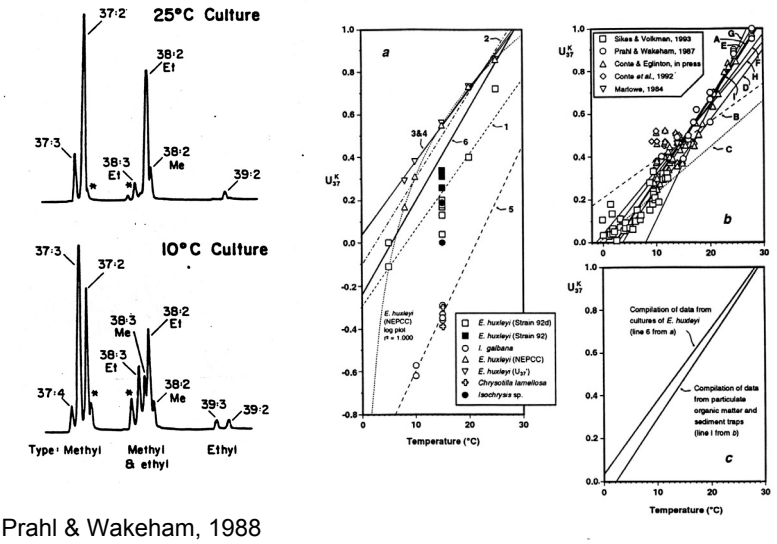

Prahl & Wakeham, 1988

Alkenone Unsaturation as an Indicator of SST

Fundamental relationship

- A decrease in temperature leads to an increase in the degree of unsaturation
- Initial ratio:

$$U^{K}_{37} = [C37:2]-[C37:4]/[C37:2+C37:3+C37:4]$$

(Brassell et al., 1986)

- Modified to:

$$U^{K}_{37}' = [C37:2]/[C37:2 + C37:3]$$

(Prahl and Wakeham, 1987)

- *Ratio can be measured very precisely (GC-FID)*

Calibration

- Most commonly used:

$U^{K}_{37}' = 0.033T + 0.043$ (Prahl and Wakeham, 1987)

$U^{K}_{37}' = 0.033T + 0.044$ (core-top calibration of Muller et al. 1998).

- Accuracy of SST estimation: ± 1°C (in open ocean, temperate and sub-polar waters)

Measurement of Alkenone Unsaturation

Conventional method

- Solvent extraction
- Column chromatography or Thin layer chromatography
- Gas Chromatography

Purification methods

- Silylation
- Saponification
- Transesterification
- Solid phase extraction

Novel detection methods

- Short-column gas chromatography-CI mass spectrometry
- DEI-HRMS (DT-MS)
- GC/TOF-MS
- GCxGC

Typical analytical scheme

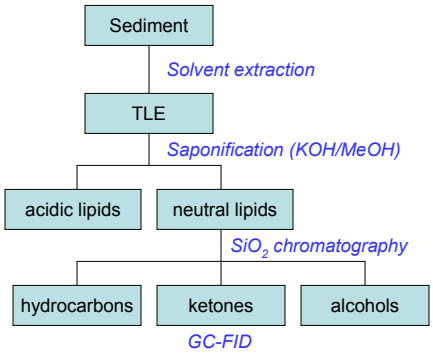

Selection of purification steps depends on whether there are additional target analytes or if isotopic information on alkenones is desired.

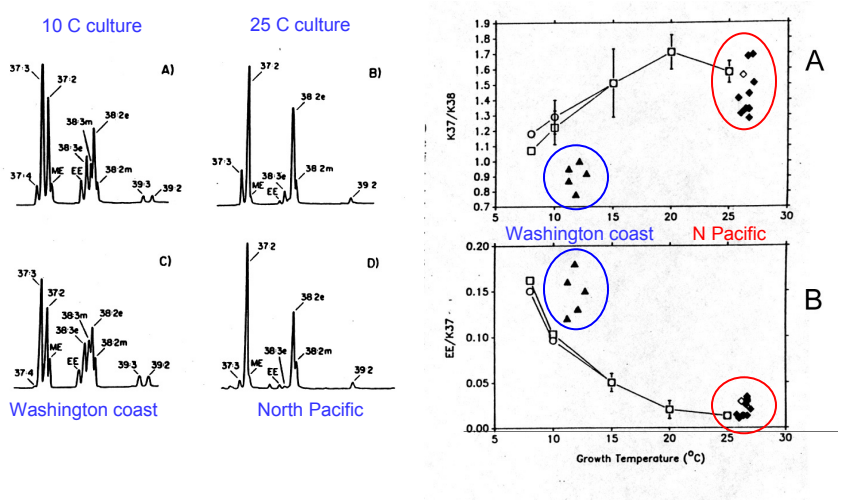

Prahl et al., 1988

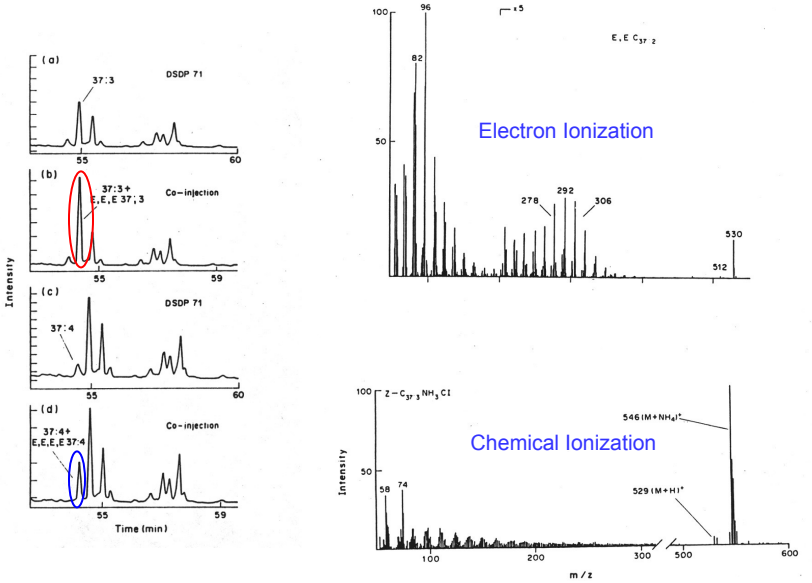

Rechka & Maxwell, 1988

The alkenone story - birth of a novel paleoceanographic tool

1989

Poynter et al. 1989

- Analysis of "stacked" core records confirmed Uk37 vs d18O relationship

1990

Marlowe et al. (1990)

- Micropaleontological and molecular data suggests genera belonging to family Gephyrocapsaceae were all potential sources of alkenones in sediments deposited since Eocene (45Ma). Cretaceous samples - ancestors of this family

McCaffrey et al. (1990)

- Alkenone Uk37 found to record short-term climatic varations (El Nino events) in Peru margin sediments over last 300yrs.

Jasper and Hayes (1990)

- δ13C of alkenones used for reconstruction of pCO2 over last 70kyr from quaternary sediments (Pygmy basin, Gulf of Mexico) - correspondence with Vostok ice core record.

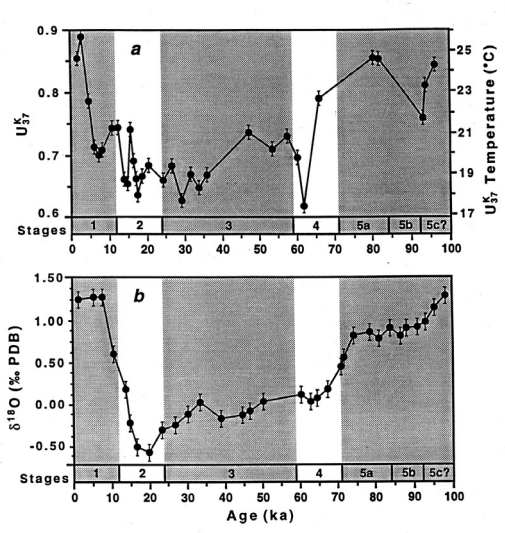

Molecular stratigraphy of Pigmy Basin sediments, Gulf of Mexico (Jasper and Gagosian, 198?)

The alkenone story - birth of a novel paleoceanographic tool

1992

Conte et al. (1992)

- Calibration of alkenone and alkyl alkenoate distributions in Eastern North Atlantic (high latitude, cold water).
- Assessment of diagenetic alteration in water column and in sediments indicates SST signature preserved, despite significant compound loss
- Definition of new parameter based on alkyl alkanoate abundance, “AA36”

Kennedy and Brassell, (1992)

- Annual climatic variations over 20th century interpreted from Uk37 in Santa Barbara basin laminated sediments

Freeman and Wakeham, (1992)

- Analysis of Uk37 in Black Sea sediments indicates a different calibration required.
- Different d13C values for C37:4 relative to C37:2 and C37:3 - different sources?

Water column-based SST calibration

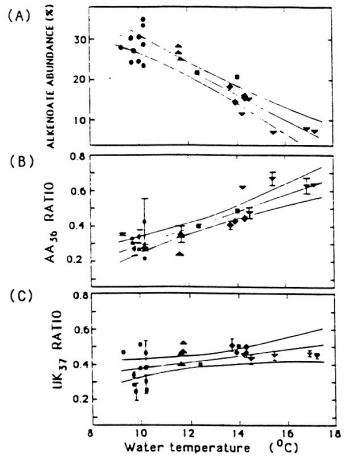

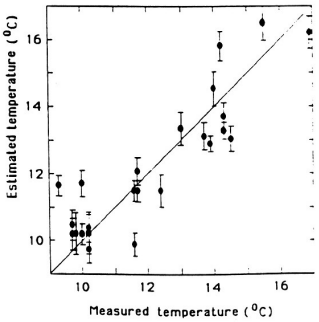

Conte et al., 1992

Alkenone-based SST records of El Nino

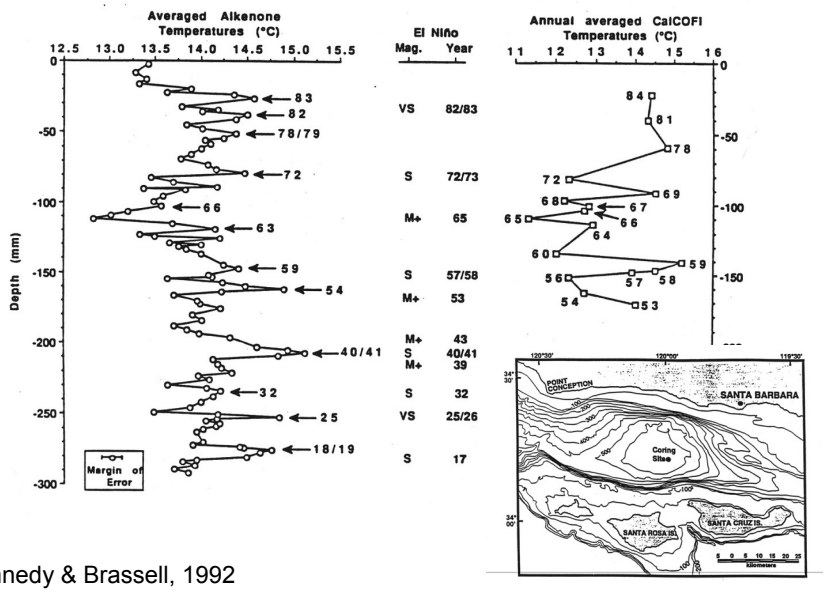

Kennedy & Brassell, 1992

Alkenones in the Black Sea (Freeman and Wakeham, 1992)

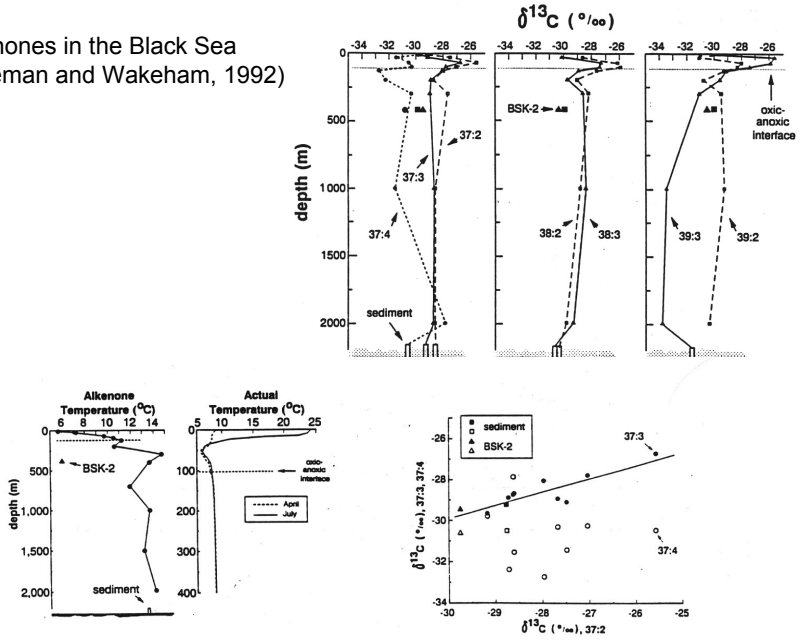

The alkenone story - birth of a novel paleoceanographic tool

1993

Jasper and Hayes, (1993)

- d13C of alkenones used to estimated fraction of marine carbon in Quaternary sediments.
- *Rostek et al. (1993)*
- Application of coupled Uk37 and d18O records to estimate salinity.
- *Sikes and Volkman (1993)*
- Extension of Uk37 temperature calibration below 11 deg C.

1995

Volkman et al. (1995)

- Identification of alkenones in *Gephyrocapsa oceanica*.

1998

Muller et al. (1998)

- "Global" core top Uk37 calibration.

1999

Sachs et al. (1999)

- Very high resolution Uk37 record for NW Atlantic across MIS-3.

Reconstructing sea surface temperature and salinity using alkenone and $\delta^{18}O$ records

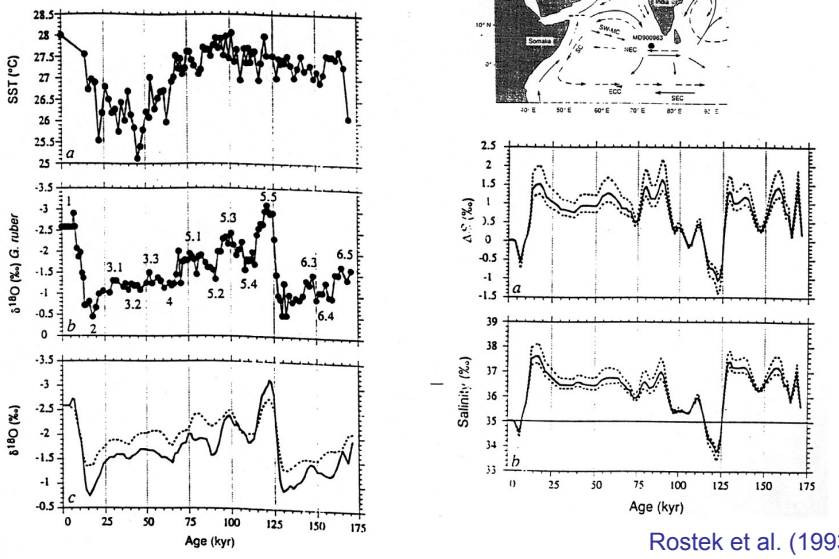

Rostek et al. (1993)

Calibration of alkenone unsaturation ratios for paleotemperature estimation in cold polar waters

Sikes & Volkman (1993)

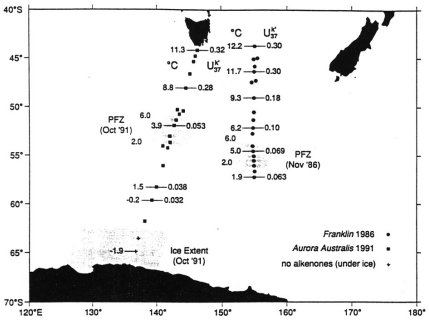

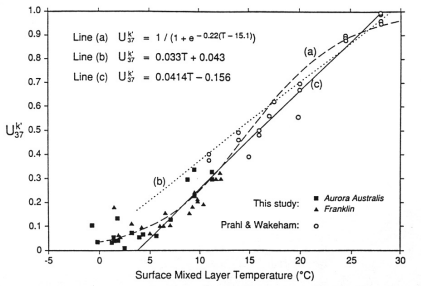

Alkenones in *Gephyrocapsa oceanica*

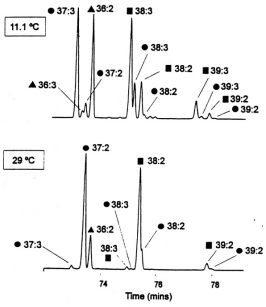

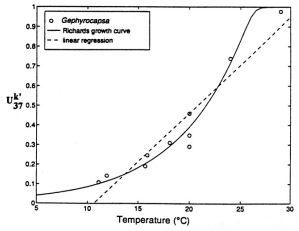

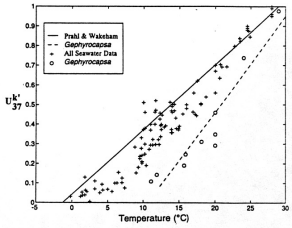

Global core-top calibration of U^{K}_{37}' vs SST

(Muller et al., 1998)

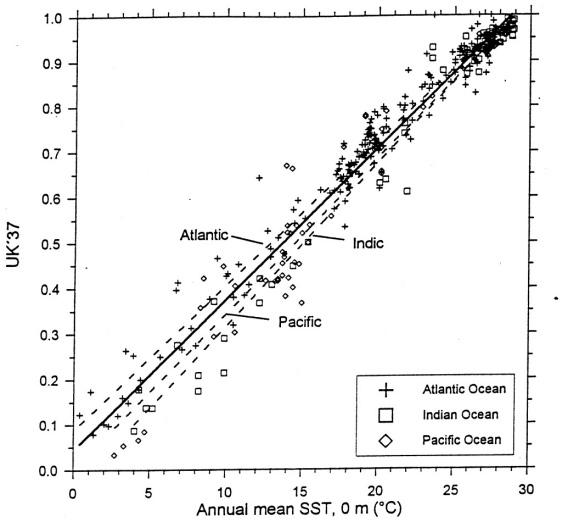

The alkenone story - birth of a novel paleoceanographic tool

2000
Benthien and Muller 2000
- Evidence for lateral transport of alkenones.

2001
Zink et al.
- Temperature relationship observed in alkenones from freshwater lakes

2001
Xu et al.
- Identification of a novel ($C_{36:2}$) alkenone in Black Sea sediments

2002
Ohkouchi et al. (2002)
- Temporal offsets observed between alkenones and planktonic foraminifera in a marine sediment drift.

2005
Englebrecht & Sachs (2005)
- Hydrogen isotopic measurements on alkenones -provenance, salinity indicators

Seasonal variations in depth of alkenone production

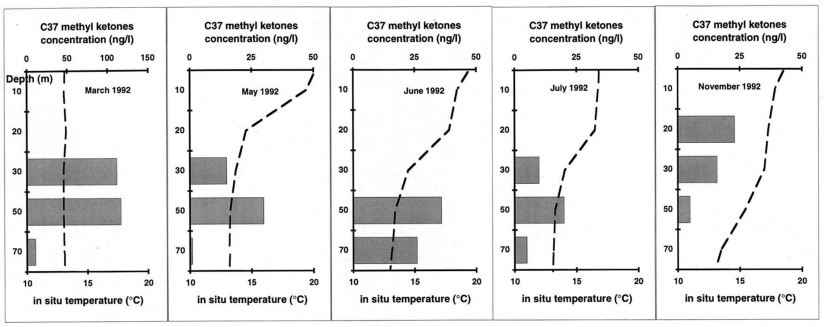

Lateral transport of alkenones to the Argentine Basin

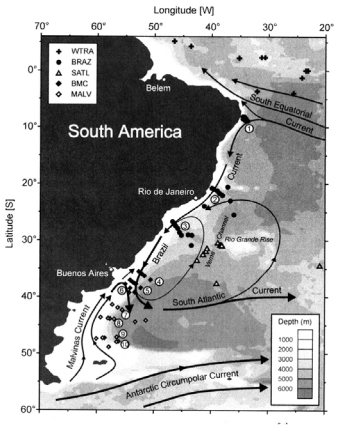

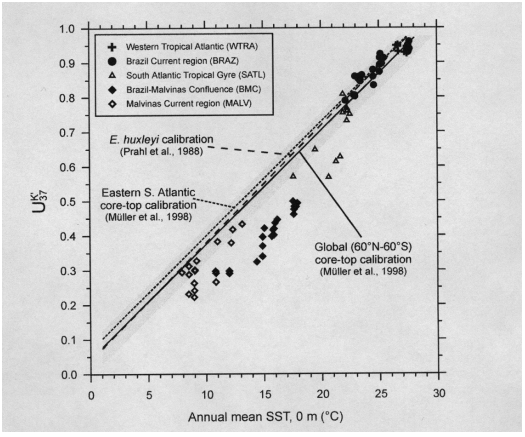

Benthien & Muller, 2000

Alkenones in freshwater lakes

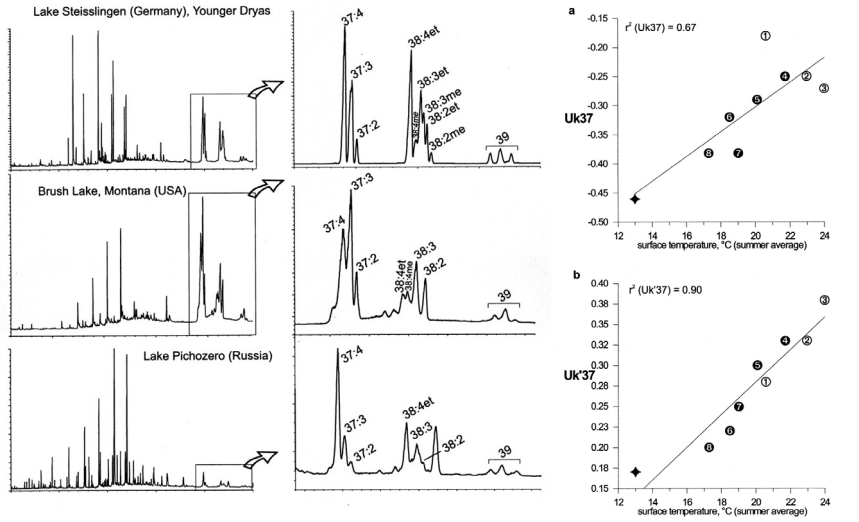

Zink et al. 2001

A novel alkenone in Black Sea sapropel (Unit II)

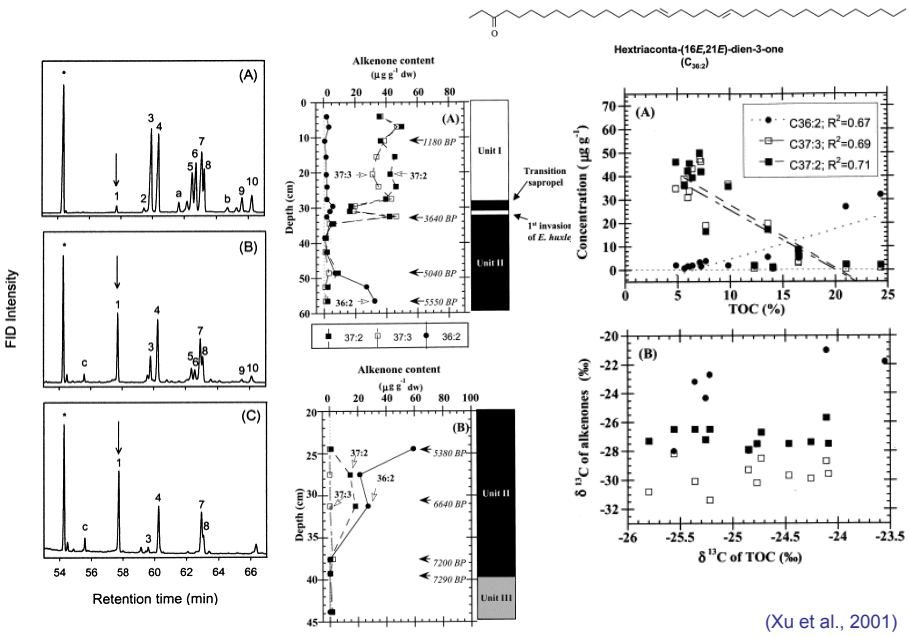

(Xu et al., 2001)

Molecular stratigraphic records from the Alboran Sea (western Mediterranean)

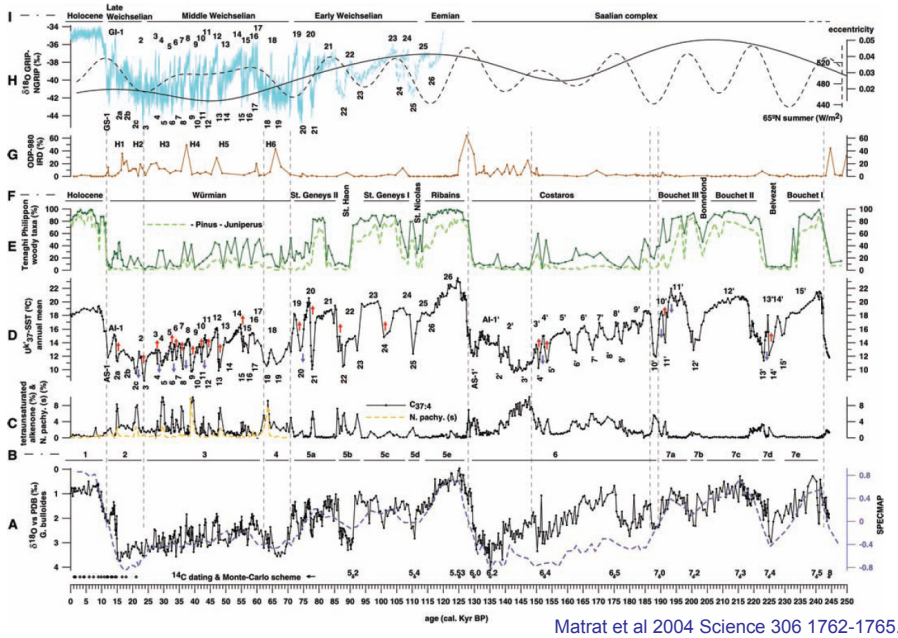

Matrat et al 2004 Science 306 1762-1765.

Important Remaining Questions

- How are alkenones biosynthesized and what their physiological role?.
- What are the spatial and temporal productivity patterns for alkenone producers.
  - Coastal vs. open ocean settings.
  - Vertical distribution in the water column.
- Time-periods pre-dating *E. hux.*
- What are the reaction pathways by which alkenones are degraded?
- Is the ketone group or the unsaturation the initial site of attack?
- Influences of preservation under oxic v anoxic conditions?
- Importance of sediment redistribution processes on alkenone/molecular records.
  - Lateral advection (drift deposits).
  - Differential bioturbation.

Emergence of a new molecular SST proxy – TEX_{86}

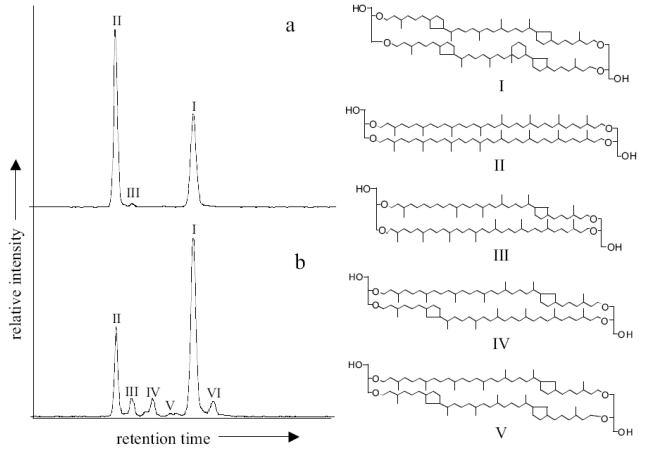

Fig. 1. HPLC/MS base peak chromatograms of (a) a surface sediment from Halley Bay Station (Antarctica), (b) a surface sediment from the Arabian Sea. Roman numerals indicate structures drawn besides. GDGT-0 **II** and GDGTs **III**–**V** were identified based on standards obtained from a lipid extract of *Sulfolobus solfaticarus* with known composition [14]. Crenarchaeol **I** was identified by isolation and analysis by high-field ^{13}C-NMR [15]. GDGT **VI** has an, as yet, unknown structure but contains five rings, as deduced from its positive ion APCI mass spectrum. Furthermore, HI cleavage of an isolated fraction of a sediment extract containing high amounts of **VI** released carbon skeletons with similar mass spectral features as those of carbon skeletons released from **I**. Thus, it is thought that **VI** is an isomer of **I**.

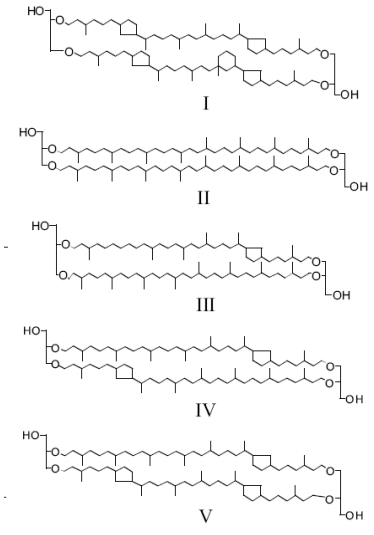

$$TEX_{86} = \frac{([\mathbf{IV}] + [\mathbf{V}] + [\mathbf{VI}])}{([\mathbf{III}] + [\mathbf{IV}] + [\mathbf{V}] + [\mathbf{VI}])} \quad (1)$$

$$TEX_{86} = 0.015T + 0.28 \; (r^2 = 0.92) \quad (2)$$

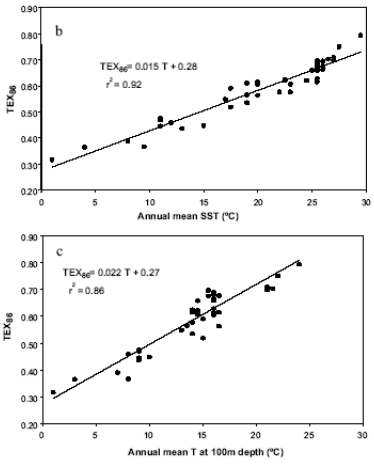

Schouten et al 2002 EPSL 265-274.

Emergence of a new molecular SST proxy – TEX_{86}

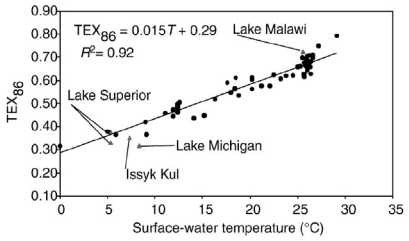

Figure 2. Correlation of TEX_{86} with mean annual sea-surface temperatures (SSTs) in marine samples (solid dots) and mean annual lake-surface temperatures for lacustrine samples (gray triangles). There are two identical points for Lake Malawi.

Powers et al. 2004

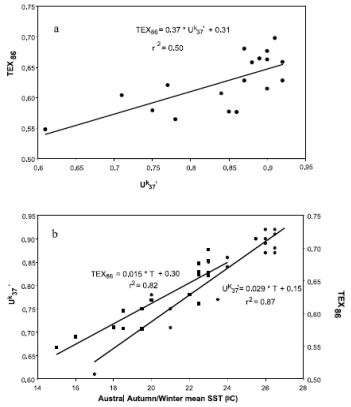

Fig. 4. Correlation of the geochemical proxies in core-top sediments with SST in the Angola Basin. Graph a shows the correlation of TEX_{86} (defined as in Eq. 1) with $U^{K'}_{37}$. Graph b shows correlations of $U^{K'}_{37}$ with austral autumn mean SST and TEX_{86} with austral winter mean SST from Angola Basin core-top sediments with SSTs determined from [21] with a precision of 0.5°C.

Schouten et al. 2004

Potential advantages of TEX_{86} proxy

- Applicable deeper in geologic record
- Applicable at higher end of temperature spectrum.
- Near ubiquitous signal
- Applicable in sediments depauperate in, or corrosive to, carbonate microfossils.
- Applicable in marine & freshwater environments.

Arctic Ocean temperatures during the Paleocene-Eocene thermal maximum (~ 55 Ma)

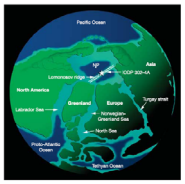

Figure 1 | Location of IODP Hole 302-4A within the palaeogeographic reconstruction of the Arctic Basin at late Palaeocene–early Eocene times. The figure is modified from ref. 24. NP, North Pole.

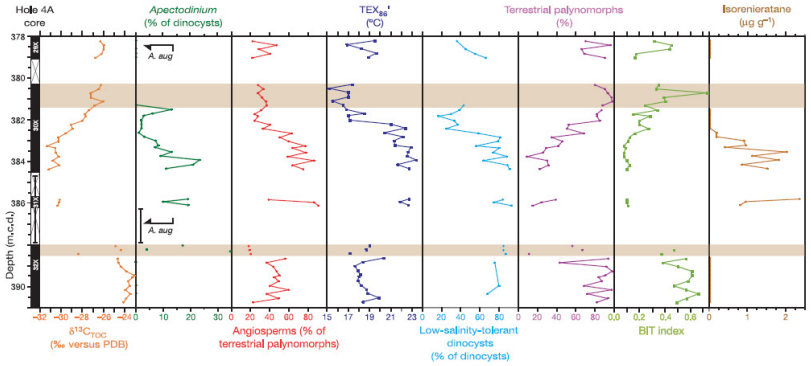

Figure 2 | Core recovery and palynological and geochemical results across the PETM of IODP Hole 302-4A. Core 31X was plotted 100 cm lower than m.c.d.[5] for illustration purposes. Error bars connected to Core 31X in the recovery column indicate the uncertainty of its stratigraphic position (see Supplementary Information). Orange bars indicate intervals affected by drilling disturbance. Stable carbon isotopes are expressed relative to the PeeDee Belemnite standard. Low-salinity-tolerant dinocysts comprise *Senegalinium* spp., *Cerodinium* spp., and *Polysphaeridium* spp., while *Membranosphaera* spp., *Spiniferites ramosus* complex, and *Areoligera-Glaphyrocysta* cpx. represent the typical normal marine species[25] (Supplementary Fig. S–1). Arrows and *A. aug* indicate the first and last occurrences of dinocyst *Apectodinium augustum*.

Sluijs et al 2006 Nature 441 610-613

Pacific Ocean SSTs during Cretaceous Anoxic Events

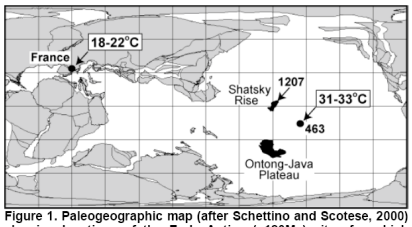

Figure 1. Paleogeographic map (after Schettino and Scotese, 2000) showing locations of the Early Aptian (~120Ma) sites for which temperature data are available (France: Pucéat et al., 2003; DSDP Site 463: Schouten et al., 2003). The range of temperatures from Site 463 excludes the sample reported with a temperature of 27 °C, a value now thought suspect because of maturity.

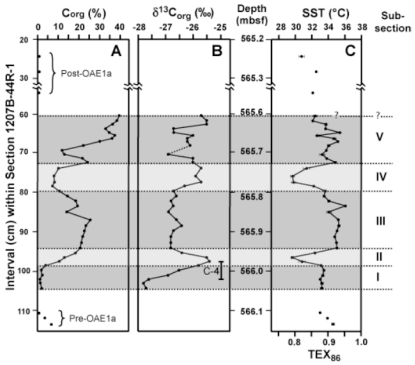

Figure 2. Depth profiles of biogeochemical and paleotemperature data for the OAE1a sequence recovered from ODP Site 1207. The recovered sequence corresponding to OAE1a is shaded, with subsections (I to V) discussed in text designated by the intensity of shading. A: organic carbon content (%). B: carbon isotopic composition of the organic matter (‰ Vienna PDB), with the positive excursion assigned as C-4 (Dumitrescu and Brassell, in press; Menegatti et al., 1998). C: sea surface temperatures (SSTs) based on the TEX_{86} proxy.

Potential complications to the TEX_{86} proxy

- Origin (water depth) of temperature signal
- Species effects
- Mode of transmission of the signal to the sediments
- Interferences from terrestrial compounds
- Accuracy of temps recorded

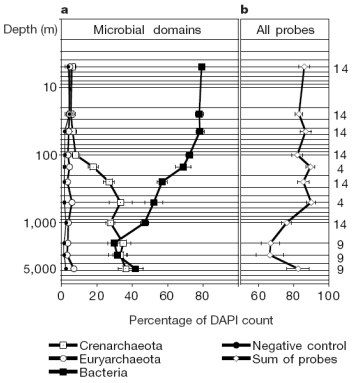

Figure 2 Mean annual depth profiles of microbial domains in the North Pacific subtropical gyre. Numbers are percentages of bacteria and archaea as compared to total microbial abundance at each depth. Total cell abundance was assessed using the DAPI nucleic acid stain. Bacteria and archaea were enumerated using whole-cell rRNA targeted fluorescent *in situ* hybridization with fluorescein-labelled polynucleotide probes. Data are averages of up to 14 roughly monthly samplings over a 1-yr period at the Hawai'i Ocean Time-series station, ALOHA. Error bars show standard error of mean; note column for total sample size at each depth. See also Supplementary Information. **a**, Depth profiles for bacteria (solid squares), pelagic crenarchaeota (open squares), pelagic euryarchaeota (open circles), and a non-specific control probe ('negative', solid circles). **b**, Depth profile of the sum of relative abundances of bacteria, pelagic crenarchaeota and pelagic euryarchaeota (open diamonds). Relative abundances of bacteria and both archaeal groups were summated at each depth and negative control data were subtracted.

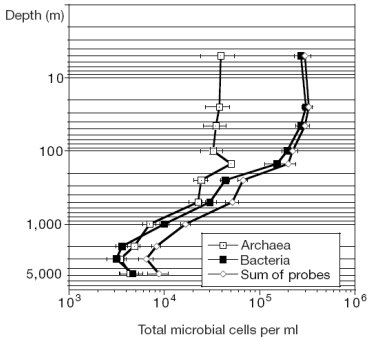

Figure 3 Mean annual depth profiles of microbial domains in the North Pacific subtropical gyre. Numbers are total cell abundances of bacteria and archaea (pelagic crenarchaeota and euryarchaeota combined). Bacteria and archaea were enumerated using whole-cell rRNA targeted fluorescent *in situ* hybridization with fluorescein-labelled polynucleotide probes. Data are averages of up to 14 roughly monthly samplings over a 1-yr period at the Hawai'i Ocean Time-series station, ALOHA. See also Supplementary Information.

Karner et al 2001 Nature

A novel proxy for terrestrial organic matter in sediments based on branched and isoprenoid tetraether lipids

E.C. Hopmans et al. / Earth and Planetary Science Letters 224 (2004) 107–116

*I. 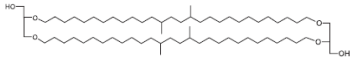

*II. 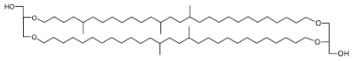

*III. 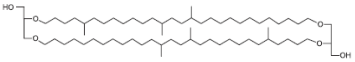

**IV. 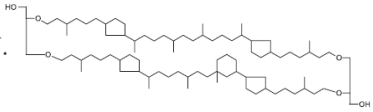

The Branched and Isoprenoid Tetraether ("BIT") index:

$$\mathrm{BIT} = \frac{[\mathrm{I} + \mathrm{II} + \mathrm{III}]}{[\mathrm{I} + \mathrm{II} + \mathrm{III}] + [\mathrm{IV}]}$$

* Derived from anaerobic soil bacteria

** Derived from derived from non-thermophillic crenarchaeota

Influence of terrestrially-derived GDGTs on TEX_{86}

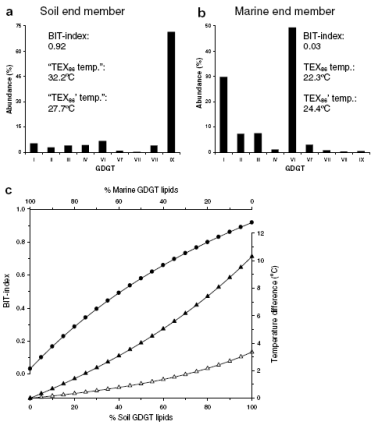

Fig. 5. Hypothetical binary mixing model for equatorial Atlantic region composed of (a) an end member representing average GDGT distribution in the African soils, and (b) an end member representing the GDGT distribution in a marine sediment sample from core GeoB 4901 (Niger deep sea fan). Graph (c) shows with different mixing ratios the positive temperature difference from the original marine end member value according to the TEX_{86} proxy (black triangles) and the TEX_{86}' proxy (white triangles) with the accompanying BIT indices (black dots).

$$\text{BIT index} = \frac{[\mathrm{VII} + \mathrm{VIII} + \mathrm{IX}]}{[\mathrm{VII} + \mathrm{VIII} + \mathrm{IX}] + [\mathrm{VI}]} \quad (1)$$

The TEX_{86} was calculated as follows (Schouten et al., 2002):

$$\mathrm{TEX}_{86} = \frac{[\mathrm{III} + \mathrm{IV} + \mathrm{VI}']}{[\mathrm{II} + \mathrm{III} + \mathrm{IV} + \mathrm{VI}']} \quad (2)$$

The TEX_{86} was converted to temperature according to the empirically derived formula given by Schouten et al. (2002):

$$T\ (^{\circ}\mathrm{C}) = \frac{\mathrm{TEX}_{86} - 0.28}{0.015} \quad (3)$$

An alternative TEX_{86} proxy, the TEX_{86}', applied by Sluijs et al. (2006) to reduce the influence of terrestrially derived isoprenoid GDGTs, is defined as:

$$\mathrm{TEX}_{86}' = \frac{[\mathrm{III} + \mathrm{VI}']}{[\mathrm{II} + \mathrm{III} + \mathrm{VI}']} \quad (4)$$

The TEX_{86}' was converted to temperature with the formula given by Sluijs et al. (2006):

$$T'\ (^{\circ}\mathrm{C}) = \frac{\mathrm{TEX}_{86}' - 0.20}{0.016} \quad (5)$$

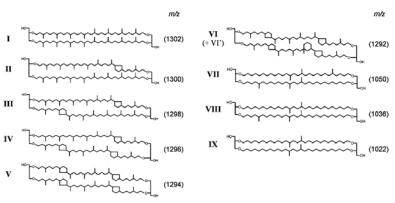

Weijers et al 2006 OG

Parameterizing compositional variability within branched GDGTs

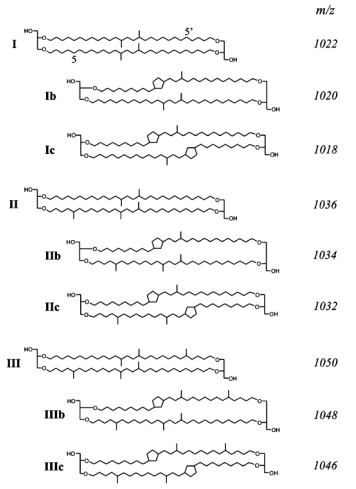

Fig. A1. Chemical structures of the branched glycerol dialkyl glycerol tetraether (GDGT) membrane lipids discussed in the text.

Methylation index of branched tetraethers (MBT)

$$\mathrm{MBT} = \frac{[\mathbf{I} + \mathbf{Ib} + \mathbf{Ic}]}{[\mathbf{I} + \mathbf{Ib} + \mathbf{Ic}] + [\mathbf{II} + \mathbf{IIb} + \mathbf{IIc}] + [\mathbf{III} + \mathbf{IIIb} + \mathbf{IIIc}]}$$

Cyclisation ratio of branched tetraethers (CBT)

$$\mathrm{CBT} = -\log\left(\frac{([\mathbf{Ib}] + [\mathbf{IIb}])}{([\mathbf{I}] + [\mathbf{II}])}\right)$$

Weijers et al 2007 GCA 71 703–713

Calibration of branched GDGT indices

CBT = 3.33 - 0.38 * pH (R^2 = 0.70).

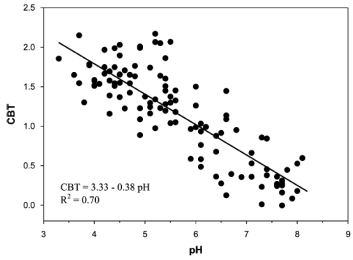

Fig. 8. Calibration plot of the cyclisation ratio of branched tetraethers (CBT) in soils vs. soil pH.

MBT = 0.122 + 0.187 * CBT + 0.020 * MAT (R^2 = 0.77).

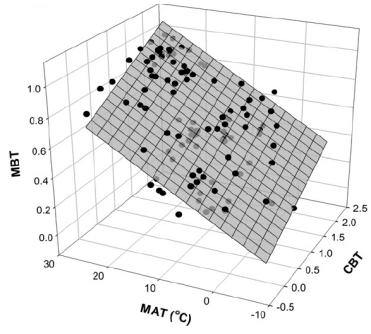

Fig. 9. 3-D calibration plot of the methylation index of branched tetraethers (MBT) in soils vs. the cyclisation ratio of branched tetraethers (CBT) in soils and annual mean air temperature (MAT).

Weijers et al 2007 GCA 71 703–713

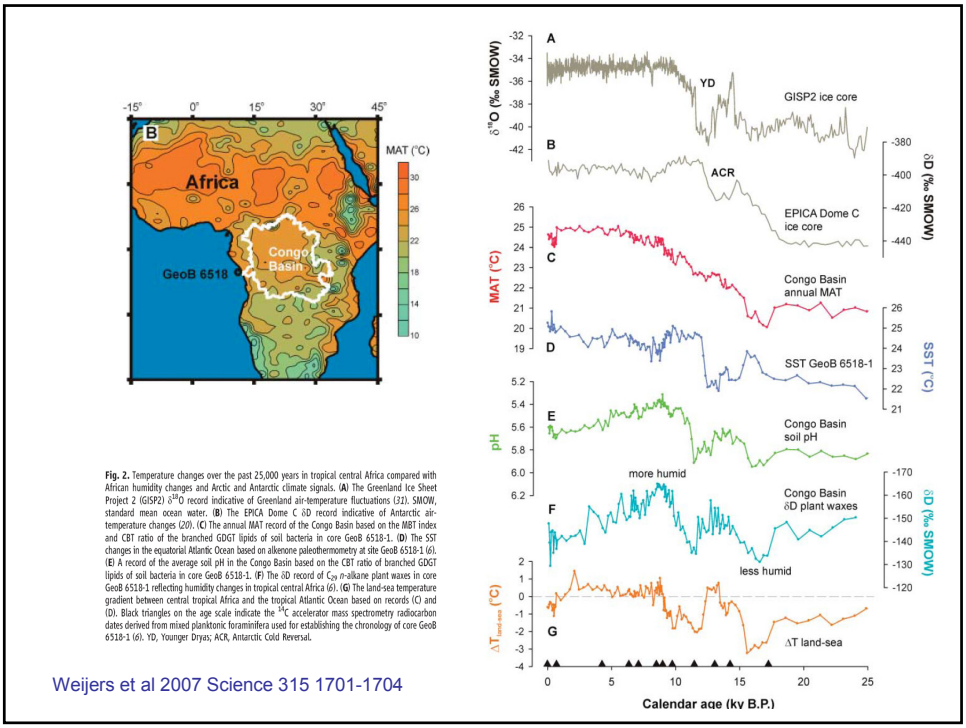

Fig. 2. Temperature changes over the past 25,000 years in tropical central Africa compared with African humidity changes and Arctic and Antarctic climate signals. (**A**) The Greenland Ice Sheet Project 2 (GISP2) $\delta^{18}O$ record indicative of Greenland air-temperature fluctuations (*32*). SMOW, standard mean ocean water. (**B**) The EPICA Dome C δD record indicative of Antarctic air-temperature changes (*20*). (**C**) The annual MAT record of the Congo Basin based on the MBT index and CBT ratio of the branched GDGT lipids of soil bacteria in core GeoB 6518-1. (**D**) The SST changes in the equatorial Atlantic Ocean based on alkenone paleothermometry at site GeoB 6518-1 (*6*). (**E**) A record of the average soil pH in the Congo Basin based on the CBT ratio of branched GDGT lipids of soil bacteria in core GeoB 6518-1. (**F**) The δD record of C_{29} *n*-alkane plant waxes in core GeoB 6518-1 reflecting humidity changes in tropical central Africa (*6*). (**G**) The land-sea temperature gradient between central tropical Africa and the tropical Atlantic Ocean based on records (C) and (D). Black triangles on the age scale indicate the ^{14}C accelerator mass spectrometry radiocarbon dates derived from mixed planktonic foraminifera used for establishing the chronology of core GeoB 6518-1 (*6*). YD, Younger Dryas; ACR, Antarctic Cold Reversal.

Weijers et al 2007 Science 315 1701-1704

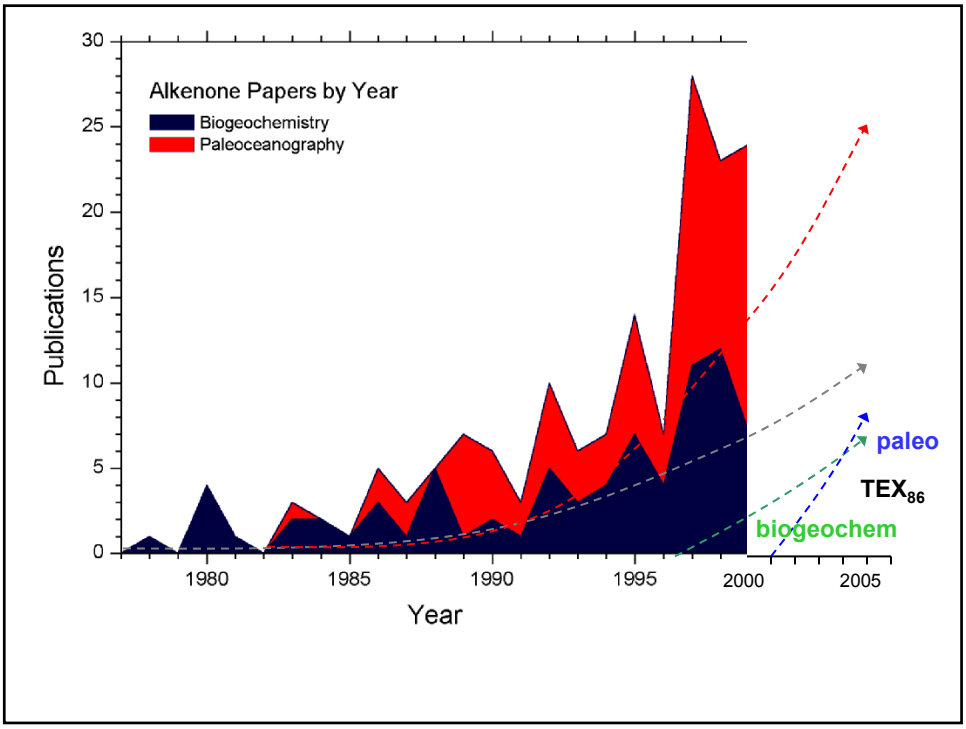

Paleoceanographic Proxy Confidence Factor Phase Chart

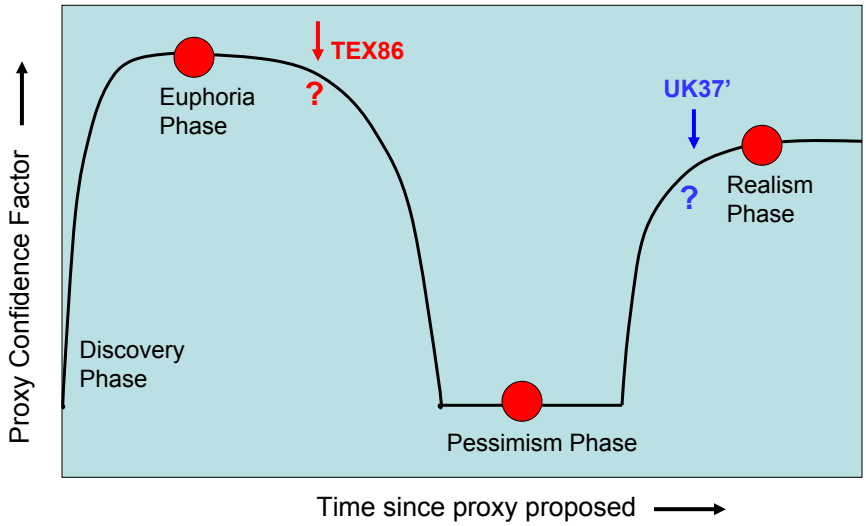

Modified after H. Elderfield